ACADEMIA ROMÂNĂ
*Revue Roumaine de Chimie*
http://web.icf.ro/rrch/

*Rev. Roum. Chim.*,
**2012**, *57*(9-10), 857-862

# STRUCTURAL AND MAGNETIC PROPERTIES OF NANOCRYSTALLINE POWDERS OF Ni – DOPED ZnO DILUTED MAGNETIC SEMICONDUCTORS SYNTHESIZED BY SOL-GEL METHOD

Teodora MĂLĂERU,[a,*] Jenica NEAMȚU[a], Cristian MORARI[a] and Gabriela SBARCEA[a,b]

[a] National Institute for Research and Development in Electrical Engineering ICPE-CA, Splaiul Unirii, No. 313, Bucharest, Roumania
[b] "Politehnica" University, Bucharest, Roumania

*Received June 14, 2011*

This paper describes the synthesis of nanocrystalline powders of ZnO:Ni diluted magnetic semiconductor synthesized by sol-gel method. The effects of Ni doping on the structural and optical properties of ZnO:Ni nanoparticles in powder samples are investigated using X-ray diffraction (XRD), Fourier transform infrared (FTIR) spectroscopy, ultraviolet-visible spectroscopy and scanning electron microscopy (SEM). The XRD and Fourier transmission infrared (FTIR) results indicated that the synthesized ZnO:Ni powders have a pure wurtzite structure without any significant change in the structure affected by substituting Zn with Ni. Optical absorption measurements showed absorption bands indicating the presence of $Ni^{2+}$ by substitution of $Zn^{2+}$. The magnetic properties of the nanocrystalline powders of ZnO:Ni have been determined by Vibrating Sample Magnetometry (VSM). Room temperature magnetization results revealed a ferromagnetic behavior for the ZnO:Ni nanocrystalline powders.

## INTRODUCTION

Diluted magnetic semiconductors (DMS) have attracted much interest in recent years because semiconductor properties can be integrated with magnetic properties to realize the objective of fabricating spin-based devices.[1,2] The researches on the synthesis and experimental characterizations of the nanostructures for diluted magnetic semiconductor (DMS) at room temperature have gained momentum. ZnO with wide band gap has been identified as a promising semiconductor material, exhibiting room temperature ferromagnetism when doped with 3d transition metal ions (V, Mn, Fe, Co, or Ni).[3-6] Ferromagnetism in transition metal-doped ZnO is theoretically predicted by Sato and Katayama-Yoshioda[7] using ab initio calculations based on local density approximation.

Various chemical methods have been developed to prepare nanoparticles of different materials of interest. Most of the ZnO crystals have been synthesized by traditional high temperature solid state method in which it is difficult to control the particle properties and also is energy consuming. ZnO nanoparticles can be prepared on a large scale at low cost by simple solution based methods, such as chemical precipitation, hydrothermal reaction, and sol-gel synthesis.

In this paper, Ni-doped ZnO nanoparticles were synthesized by sol-gel method using zinc acetate and nickel nitrate as starting precursors and propanol and monoethanolamine as solvent and stabilizer. We studied the influence of dopant ion concentration on the structure and magnetic properties of $Zn_{1-x}Ni_xO$ ($x = 0.03 \div 0.15$).

## RESULTS AND DISCUSSION

### XRD study

Fig. 1 shows the XRD diffraction patterns of nickel doped zinc oxide ($Zn_{1-x}Ni_xO$, where

* Corresponding author: teodora.malaeru@icpe-ca.ro

x = 0.03÷0.15) powder sample, sintered at a temperature of 550°C, for 2h, in air. X-ray diffraction patterns on powder indicate that the as synthesized samples have a wurtzite structure with all the peaks that correspond to ZnO agreed with the reported JCPDS card no. 36-1451 (a = b = 3.249 and c = 5.206 Å). No additional peaks corresponding to the secondary phases of nickel oxides were obtained for x = 0.03. A very small additional peak attributable to secondary phase of nickel oxide was observed when the content of Ni(x) is more than 0.05. We can conclude that the wurtzite structure of ZnO is not changed by the Ni substitution and that $Ni^{2+}$ occupies the $Zn^{2+}$ site into the crystal lattice.

Table 1 shows that the lattice constants of $Zn_{1-x}Ni_xO$ (x = 0.03÷ 0.15) are slightly smaller than those of pure ZnO, because of the difference between the ionic radius of the elements ($rZn^{2+}$ = 0.60Å and $rNi^{2+}$ = 0.55Å).

The mean crystalline size was calculated from the full-width at half maximum (FWHM) of XRD lines by using the Debye-Scherrer formula.[8] We used the most intense peaks in XRD patterns to calculate the average crystallites size (Table 2). The particles size are in the range of 40.8 to 127 nm and, as seen from Table 2, the Ni content make changes in the size of particles. For concentrations x ≥ 0.05, the size of the particles decreases linearly with increasing the content in Ni.

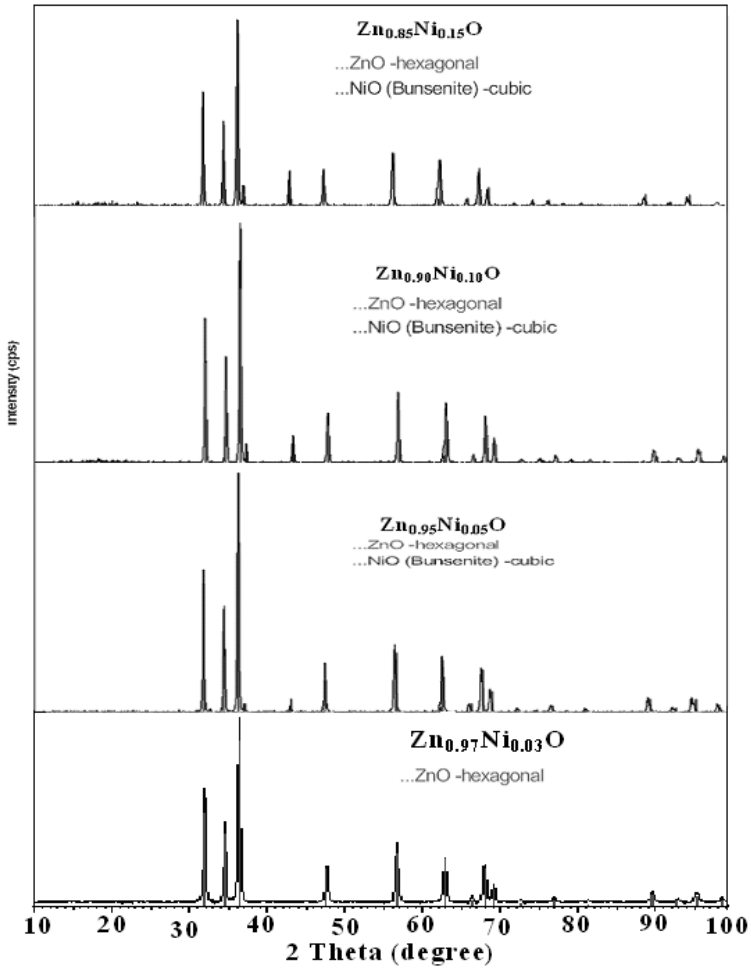


Fig. 1 – X-ray diffraction patterns of $Zn_{1-x}Ni_xO$ (X = 0.03 ÷ 0.15) powder samples.

*Table 1*

The lattice constants calculated from the XRD data of $Zn_{1-x}Ni_xO$ (x = 0.03 ÷ 0.15)

| $Zn_{1-x}Ni_xO$ (x = 0.03 ÷ 0.15) | | | | |
|---|---|---|---|---|
| x = 0 | x = 0.03 | x = 0.05 | x = 0.10 | x = 0.15 |
| a = b = 3.249 | a = b = 3.245 | a = b = 3.235 | a = b = 3.242 | a = b = 3.245 |
| c = 5.206 | c = 5.205 | c = 5.183 | c = 5.192 | c = 5.197 |

*Table 2*

Average size of particles $Zn_{1-x}Ni_xO$ (x = 0.03 ÷ 0.15)

| Concentration (x) | (hkl) | Average size of the crystallites (nm) |
|---|---|---|
| 0.03 | (1,0,0) | 48.4 |
| | (1,0,1) | 40.8 |
| 0.05 | (1,0,0) | 160 |
| | (0,0,2) | 138 |
| 0.10 | (1,0,0) | 146 |
| | (0,0,2) | 133 |
| 0.15 | (1,0,0) | 139 |
| | (0,0,2) | 127 |

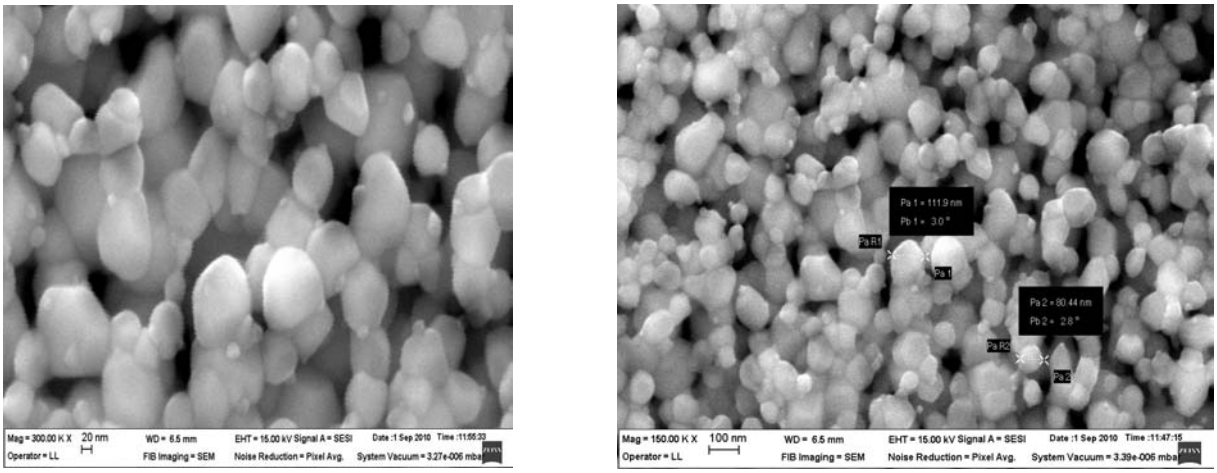

a) b)

Fig. 2 – SEM micrographs of a) $Zn_{0.97}Ni_{0.03}O$ and b) $Zn_{0.85}Ni_{0.15}O$ powder obtained at 550°C, 2h.

## SEM study

The morphology of the Ni-doped ZnO nanoparticles investigated using SEM is shown in Fig. 2. The SEM micrograph reveals that the particles are mostly spherical. The $Zn_{0.97}Ni_{0.03}O$ (Fig. 2a) and $Zn_{0.85}Ni_{0.15}O$ (Fig. 2b) nanoparticles are nanometer-sized in agreement with XRD estimations.

## FTIR study

FTIR spectra for Ni doped ZnO samples are shown in Fig. 3. Infrared transmittance spectra were used to study the vibration bands due to Zn-O bonds and changes due to Ni substitution in its structure. FTIR vibration band frequencies of Ni doped ZnO samples are given in Table 3. One can see that the vibration frequency of Zn-O bonds shows shifts. The shifts of the vibration frequency from 414, 434 and 484 $cm^{-1}$ is given by the incorporation of Ni in octahedral and tetrahedral sites existing in hexagonal-wurtzite structure. The absorption bands in the ranges from 651 to 665 $cm^{-1}$ and 430 to 446 $cm^{-1}$ are attributed to the stretching modes of Zn-O[9, 10] in the tetrahedral and octahedral coordination respectively. The bands near 700 and 860 $cm^{-1}$ are attributed to the vibration of Zn-O-Ni bonds.

*Table 3*

FTIR vibration band frequencies of Ni doped ZnO samples

| Sample | Wavenumber ($cm^{-1}$) | | | | | |
|---|---|---|---|---|---|---|
| ZnO | 414 | 434 | 484 | 665 | - | 823 |
| $Zn_{0.97}Ni_{0.03}O$ | 414 | 443 | 484 | 661 | 698 | 867 |
| $Zn_{0.95}Ni_{0.05}O$ | 417 | 430 | 499 | 651 | 791 | 867 |
| $Zn_{0.90}Ni_{0.10}O$ | 416 | - | 489 | 667 | 724 | 868 |
| $Zn_{0.85}Ni_{0.15}O$ | 413 | 443 | 499 | 661 | 697 | 867 |
| $Zn_{0.75}Ni_{0.25}O$ | 416 | 446 | 499 | 665 | 710 | 863 |

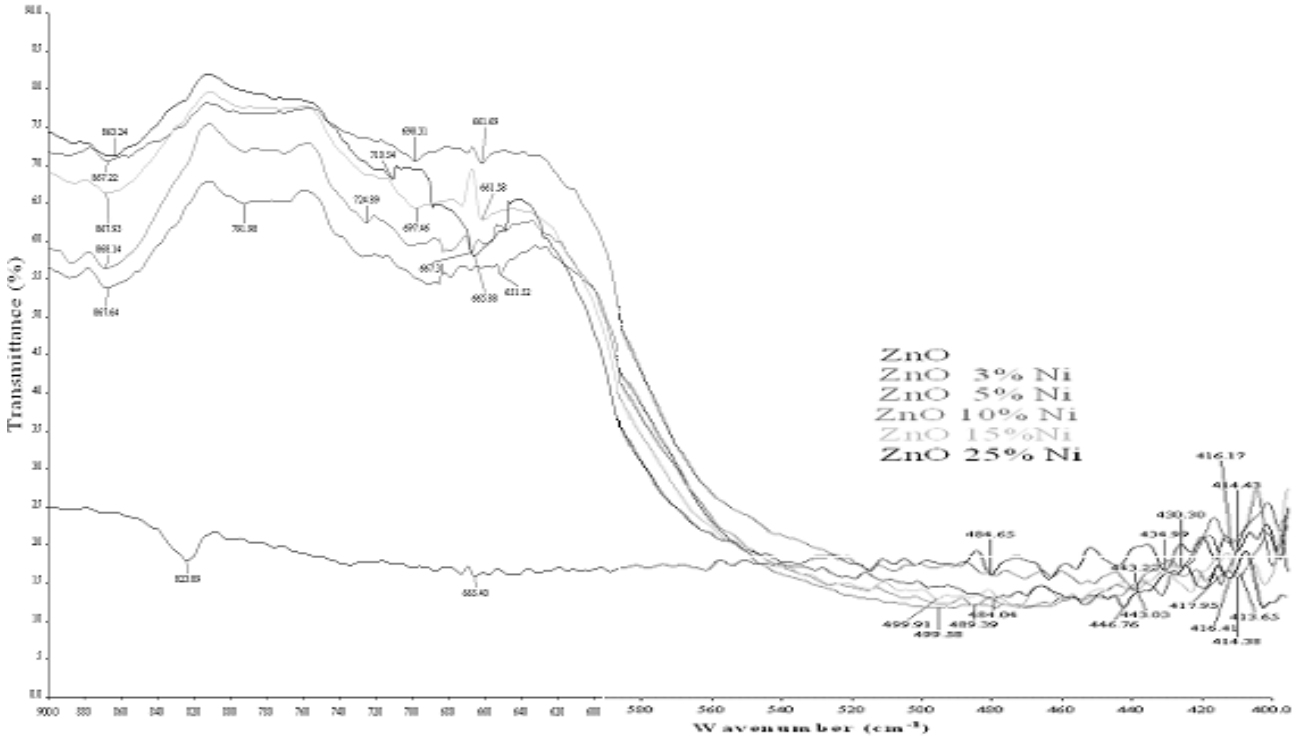


Fig. 3 – FTIR spectra of ZnO and Ni doped ZnO samples.

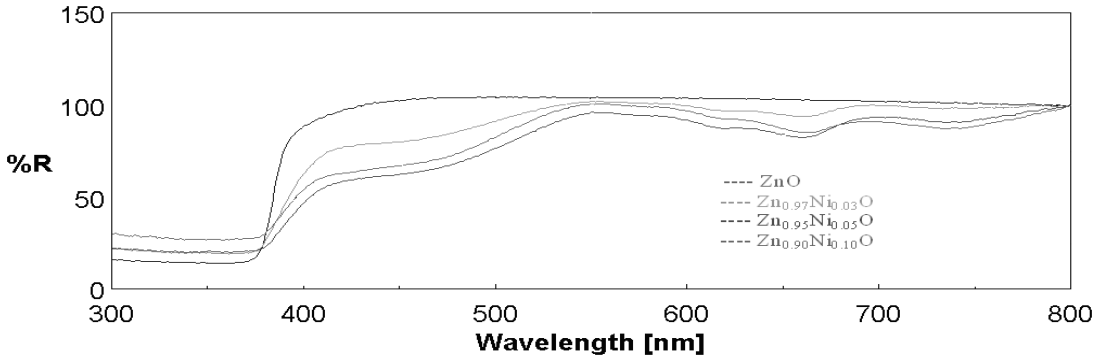


Fig. 4 – UV-vis spectra of undoped ZnO and Ni-doped ZnO samples.

## UV-vis study

The room temperature optical absorption spectra of undoped and Ni-doped ZnO samples by UV-vis spectrophotometer in the range of 200 to 800 nm are shown in Fig.4. Substitution of $Ni^{2+}$ ions in tetrahedral sites of the wurtzite structure was confirmed also by UV-vis optical spectroscopy. From Fig.4, one can see that the band edge at 400 nm of undoped ZnO is shifted towards higher wavelength side for Ni-doped ZnO samples, indicating the incorporation of Ni into the ZnO lattice.

## Magnetic study

Fig. 5 shows the magnetization versus the magnetic field measured at room temperature by Vibrating Sample Magnetometry (VSM) method for the 3 and 10% Ni-doped ZnO samples. Both samples show distinctly hysteresis loops at room temperature, which indicates that the samples have room-temperature ferromagnetism. The saturation magnetization ($M_S$) and the coercive field ($H_C$) are $2.25 \cdot 10^{-6} Am^2$ ($2.25 \cdot 10^{-3}$ emu), 12216 A/m (153.5 Oe) and $5.2 \cdot 10^{-6}$ $Am^2$ ($5.2 \cdot 10^{-3}$ emu), 7961 A/m (100 Oe) for 3 and 10% Ni-doped ZnO powder, respectively.

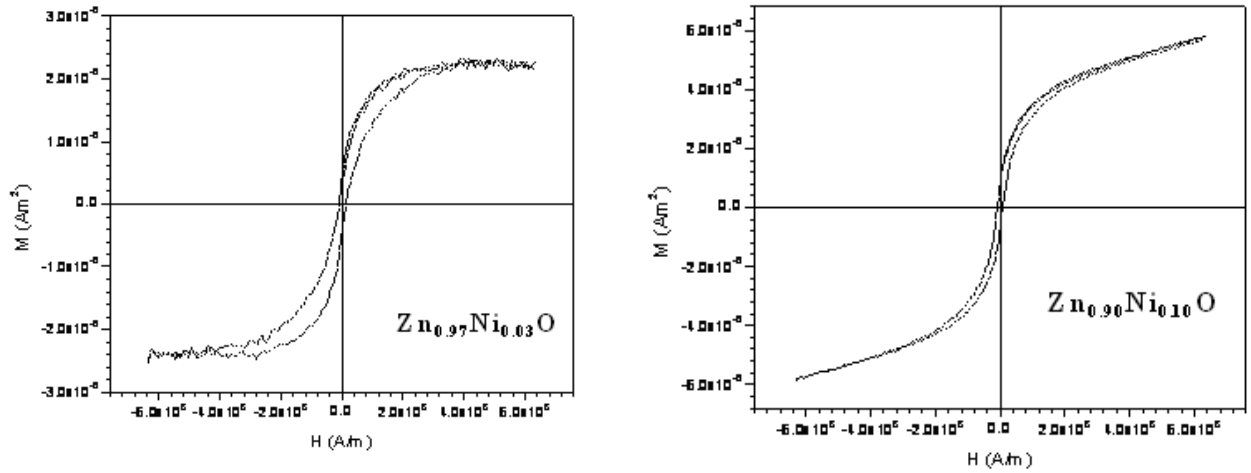


Fig. 5 – Magnetic hysteresis curves of $Zn_{0.97}Ni_{0.03}O$ and $Zn_{0.90}Ni_{0.10}O$ powder samples.

## EXPERIMENTAL

### Synthesis

$Zn_{1-x}Ni_xO$ (x = 0.03; 0.05; 0.10; and 0.15) powders were synthesized by a sol-gel method. Stoichiometric amounts of zinc acetate $Zn(CH_3CO_2)_2.2H_2O$ (Fluka 99.5%) and nickel nitrate $Ni(NO_3)_2.6H_2O$ (Aldrich 98%) were each dissolved in 20ml propanol by magnetic stirring at room temperature. Both solutions were mixed together and then monoethanolamine was added drop by drop under vigorous stirring. The resulting solution was then refluxed at 80°C for 4h until the solution was converted into a gel. The gel thus formed was dried at room temperature for 48 h. The resulting powders were than annealed at 550°C for 2h in air.

### Characterization techniques

The oxide powders were analyzed by X-ray diffraction (XRD) using Bruker-AXS type D8 ADVANCE X-ray diffractometer with Cu-$k_\beta$ radiation of 1.5406 Å, at a step of 0.04° ·$s^{-1}$ in the range 2θ = 10 – 100°. Morphology of the powder samples was investigated by FESEM-FIB (Workstation Auriga) scanning electron microscope. The vibration frequencies of bonds in sample were observed using Fourier transform infrared (FTIR) spectrometer (PERKIN ELMER Spectrum 100) in the range 400 – 4000 $cm^{-1}$. The optical absorption spectra are recorded at room temperature using ultraviolet-visible (UV-Vis-NIR) spectrophotometer (Model: V570 Able & Jasco Japonia) in the wavelength range 300-800 nm and magnetic study is done using vibrating sample magnetometer (VSM) (Model: LAKESHORE 7300). The calibration of VSM was performed using a nickel standard sample and its magnetization values as stated in the ASTM Standard A 894-89.

## CONCLUSIONS

Ni-doped ZnO ($Zn_{1-x}Ni_xO$, x = 0.03÷0.15) nanoparticles have been synthesized using a simple sol-gel method. The XRD analyses show wurtzite structure as that of ZnO for all the $Zn_{1-x}Ni_xO$ nanoparticles. When increasing Ni(x) concentration (x≥0.05), an additional diffraction peak correspondent to NiO is observed. With the increasing content of Ni, lattice parameters of doped ZnO decrease due to the ionic radius of $Ni^{2+}$ which is smaller than that of the $Zn^{2+}$ ion in tetrahedral coordination. Also, FTIR and UV-vis studies indicates that in all samples of Ni-doped ZnO, $Ni^{2+}$ ions are incorporated into the ZnO lattice. Magnetic hysteresis loops indicate the room-temperature ferromagnetism in Ni-doped ZnO nanoparticles. The Ni- doped ZnO nanoparticles of the present work having low magnetization could form the diluted magnetic semiconductors for spintronic applications.

*Acknowledgements:* This work was supported by the Roumanian National Authority of Scientific Research under the contract CNCSIS PCCE ID_76/2010 and by the Sectoral Operational Programme Human Resources Development 2007-2013 of the Roumanian Ministry of Labor, Family and Social Protection through the Financial Agreement POSDRU/88/1.5/S/60203.

## REFERENCES

1. T. Fukumura, Y. Yamada, H. Toyosaki, T. Hasegawa, H. Koinuma and M., *Appl. Surface Sci.,* **2004**, *223*, 62-67.
2. H. Ohno, *J. Magn. Magn. Mater,* **1999**, *200*, 110-129.
3. H.L. Liu, J.H. Yang, Y.J. Zhang, Y.X. Wang, M.B. Wei, D.D. Wang, L.Y. Zhao, J.H. Lang and M. Gao, *J. Mater. Sci. Mater. Electron.,* **2009**, *20,* 628-631.
4. H.W. Zhang, Z.R. Wei, Z.Q. Li and G.Y. Dong, *Mater. Lett.,* **2007**, *61,* 3605-3607.
5. S. Ghosh, P. Srivastava, B. Pandey, M. Saurav, P. Bharadwaj, D.K. Avasthi, D. Kabiraj and S.M. Shivaprasad, *Appl. Phys. A*: *Mater. Sci. & Processing,* **2008**, *90*, 765-769.
6. J. Neamtu, G. Georgescu, T. Malaeru, N.G. Gheorghe, R.M. Costescu, I. Jitaru, J. Férre, D. Macovei and C.M. Teodorescu, *Digest J. Nanomater. Bios.,* **2010**, *5*, 873-885.

7. K. Sato and H. Katayama-Yoshida, *Jpn. J. Appl. Phys,* **2000**, *39,* L555.
8. B.D. Cullity, "Elements of X-Ray Diffractions", Addison-Wesley, Reading, MA, 1978.
9. P. D. Cozzoli, M. L. Curri, A. Agostiano, G. Leo and M. Lomascolo, *J. Phys. Chem. B,* **2003**, *107,* 4756-4762.
10. R. Elilarassi and G. Chandrasekaran, *Mater. Chem. Phys.,* **2010**, *123*, 450-455.